

## Supporting Information

### Role of Particle Focusing in Resistive-Pulse Technique: Direction-Dependent Velocity in Micropores

Yinghua Qiu<sup>a,b</sup>, Ivan Vlassiouk<sup>c</sup>, Preston Hinkle<sup>a</sup>, Eugenia M. Toimil-Molares<sup>d</sup>, Alex J. Levine<sup>e,f,g</sup>, Zuzanna S. Siwy<sup>a</sup>

<sup>a</sup>Department of Physics and Astronomy, University of California, Irvine California 92697 USA

<sup>b</sup>School of Mechanical Engineering and Jiangsu Key Laboratory for Design and Manufacture of Micro-Nano Biomedical Instruments, Southeast University, Nanjing 211189, China

<sup>c</sup>Oak Ridge National Laboratory, 1 Bethel Valley Road, Oak Ridge, TN, 37831, United States

<sup>d</sup>Department of Materials Science, GSI Helmholtz Center for Heavy Ion Research, Darmstadt, Germany

<sup>e</sup>Department of Physics & Astronomy, University of California, Los Angeles 90095

<sup>f</sup>Department of Chemistry & Biochemistry, University of California, Los Angeles 90095

<sup>g</sup>Department of Biomathematics, University of California, Los Angeles 90095

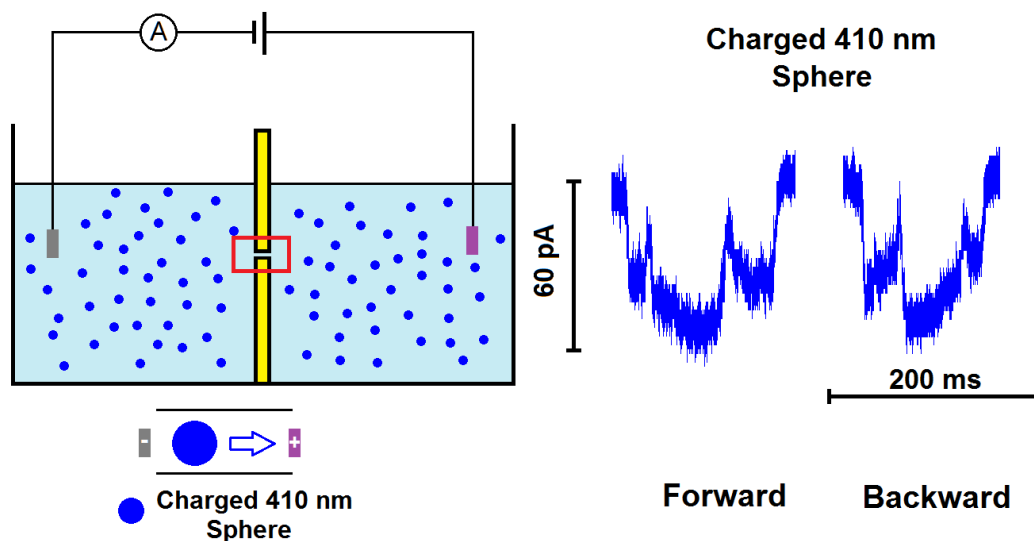
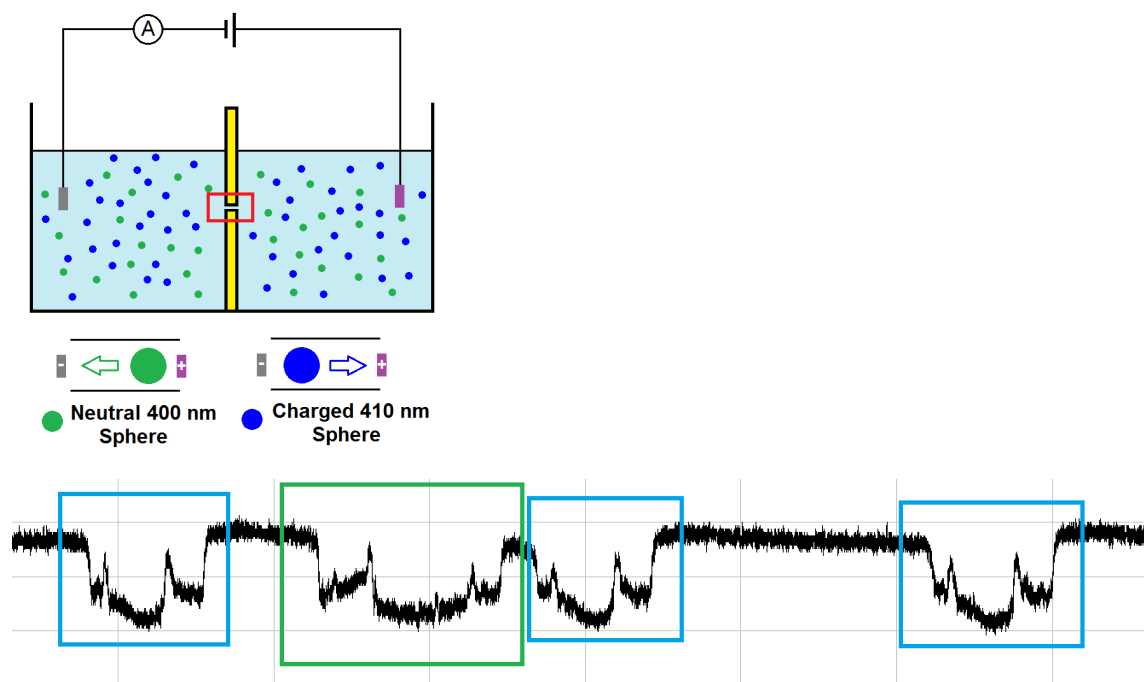
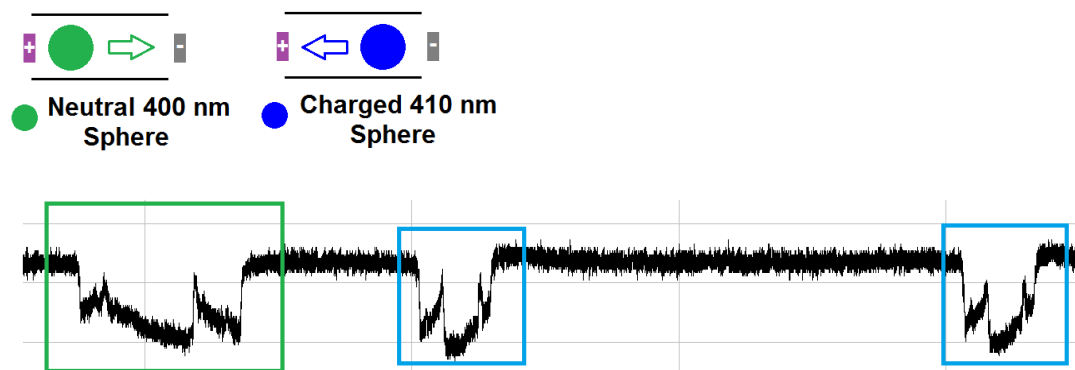


**Figure S1.** Control experiments performed with charged 410 nm particles (zeta potential of  $-33 \pm 2$  mV at 100 mM KCl, pH 10) placed on both sides of the membrane. The particles moved towards a positively biased electrode. Switching voltage polarity allowed mapping the pore 3D topography and its orientation in the conductivity cell.



*Pulses in blue boxes correspond to negatively charged 410 nm particles, translocating the pore from left-to-right (forward); pulses in green represent pulses of neutral 400 nm particles transported in the direction of electroosmosis from right-to-left (backward). Due to their opposite direction of transport, events of the two types of particles are therefore expected to be mirror images of each other, which is consistently observed here. Note, pulses of different particles have similar amplitudes consistent with their similar sizes.*



*Pulses in blue boxes correspond to negatively charged 410 nm particles, translocating the pore from right-to-left (backward); pulses in green represent pulses of 400 nm neutral particles transported in the direction of electroosmosis from left-to-right.*

**Figure S2.** Experiments performed with a mixture of particles present on both sides of the membranes. This is the same set-up as shown in Figure 1 of the main manuscript. Example current traces indicating how pulses were assigned to either neutral 400 nm or charged 410 nm particles (zeta potential of  $-33 \pm 2$  mV at 100 mM KCl, pH 10) .

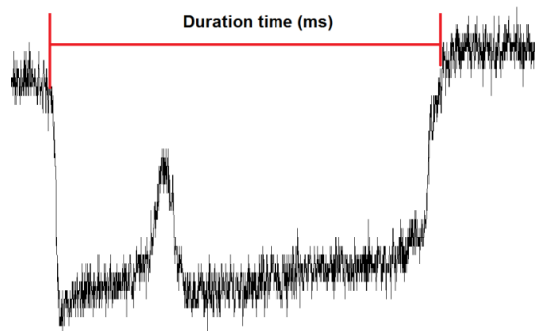


**Figure S3.** Procedure to determine transit time of individual particles. The analysis was performed with software Clampfit 10.4 (Molecular Devices, Inc.) using the threshold approach. The beginning and end of each event was established when the current exceeded 95% of the average baseline value.

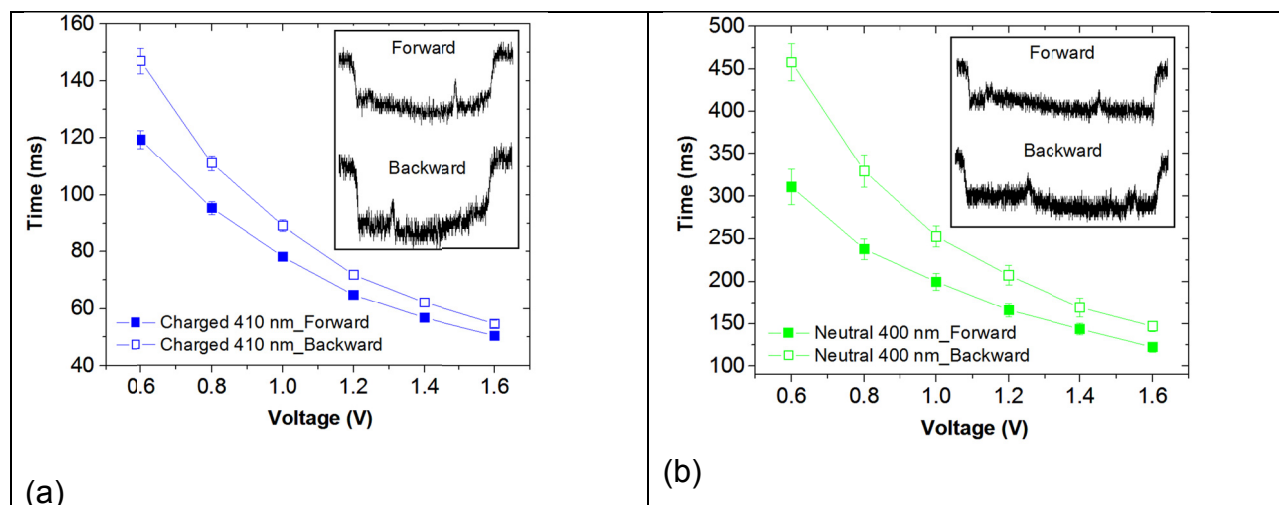


**Figure S4.** Plot of transit time versus voltage and recordings of the translocations (inset) of (a) charged 410 nm particles (zeta potential of  $-33 \pm 2$  mV at 100 mM KCl, pH 10), and (b) neutral 400 nm particles through a single polyethylene terephthalate (PET) pore with an average opening diameter of  $1.25 \mu\text{m}$  and length of  $35 \mu\text{m}$ .

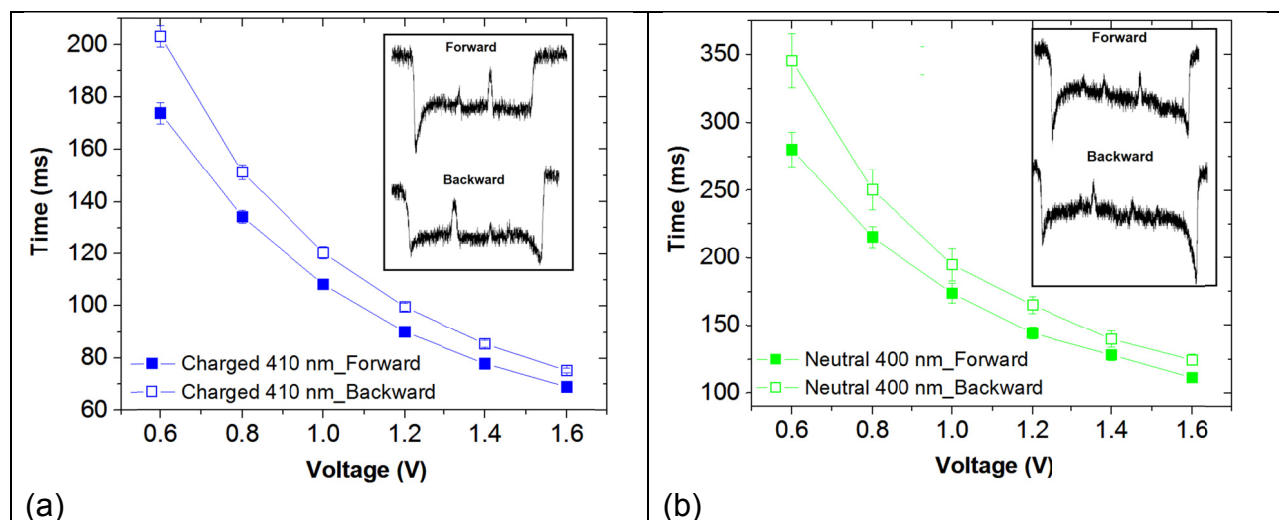


**Figure S5.** Plot of transit time *versus* voltage and recordings of the translocations (inset) of (a) charged 410 nm particles (zeta potential of  $-33 \pm 2$  mV at 100 mM KCl, pH 10), and (b) neutral 400 nm particles through a single polyethylene terephthalate (PET) pore with an average opening diameter of 1  $\mu\text{m}$  and length of 35  $\mu\text{m}$ .

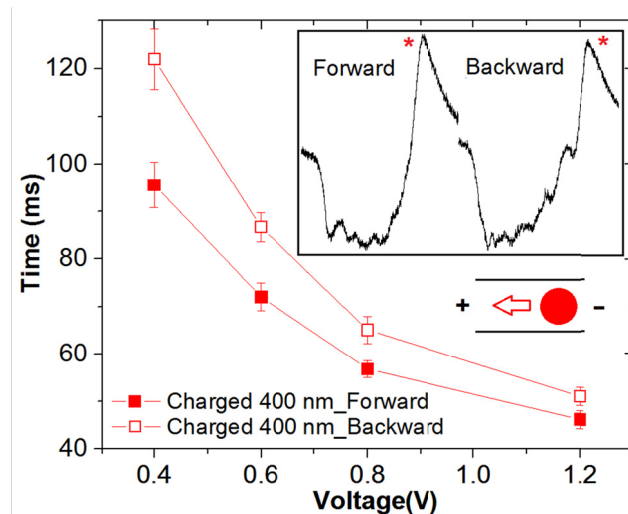


**Figure S6.** Passage time of 400 nm charged particles (zeta potential of  $-18 \pm 2$  mV at 100 mM KCl, pH 10) through an 11  $\mu\text{m}$  long PET micropore with an average opening diameter of 1.2  $\mu\text{m}$ . These particles were used in our previous publication, and exhibited an unusual dependence of their zeta potential on the solution pH.<sup>1</sup> The large current increase accompanying the particles' exit is caused by the particle induced concentration polarization. Transit time was calculated according to a similar procedure as shown in Figure S3, except that the end of each event was extended to the peak shown as asterisk\*. This allowed a consistent determination of the end of each pulse. According to our previous work, the current increase occurs when a particle is exiting the pore.<sup>2</sup>

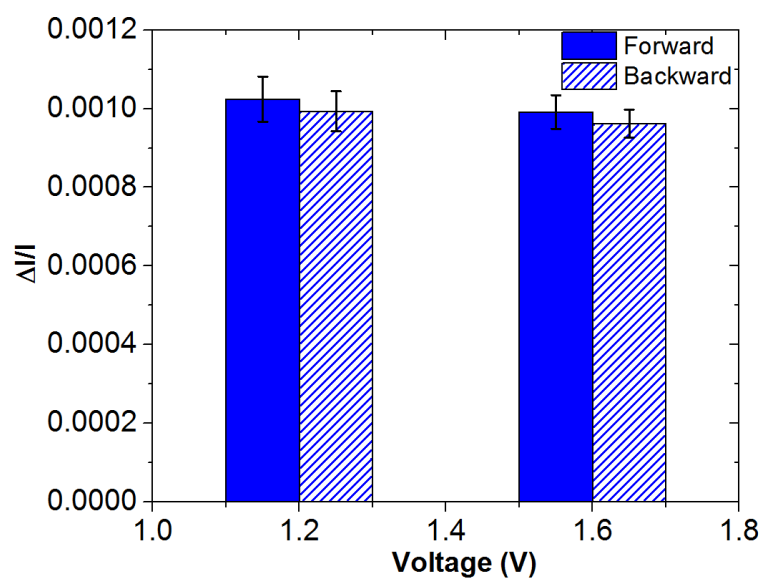
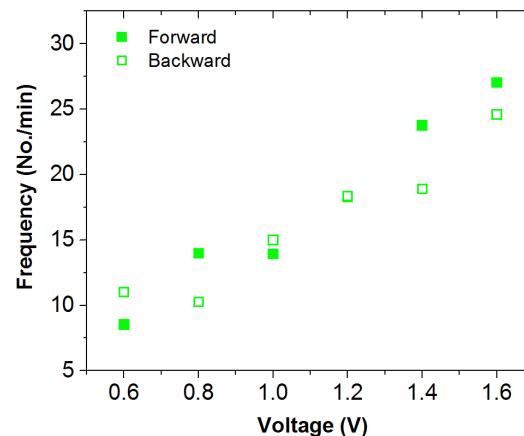
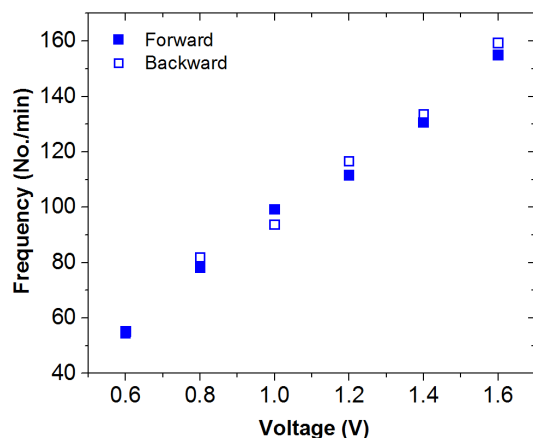
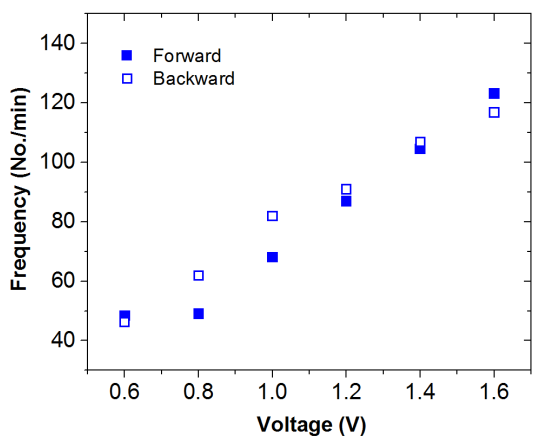


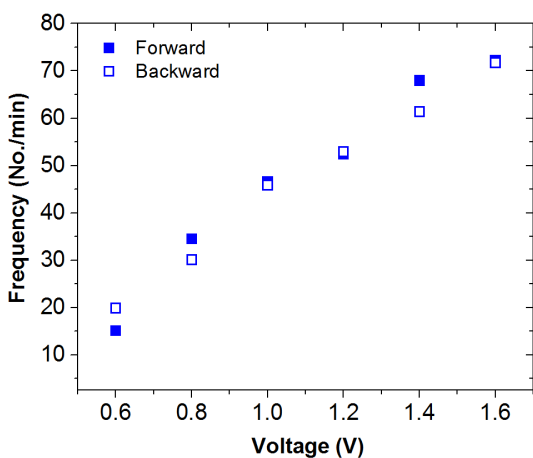
**Figure S7.** Relative current blockage caused by 410 nm charged particles (zeta potential of  $-33 \pm 2$  mV at 100 mM KCl, pH 10), passing through the narrow zones of the pore shown in Figure 3 (main manuscript) in both directions.



(a) Micropore shown in Figures 1,2



(b) Micropore shown in Figure 3



(c) Micropore shown in Figure S4

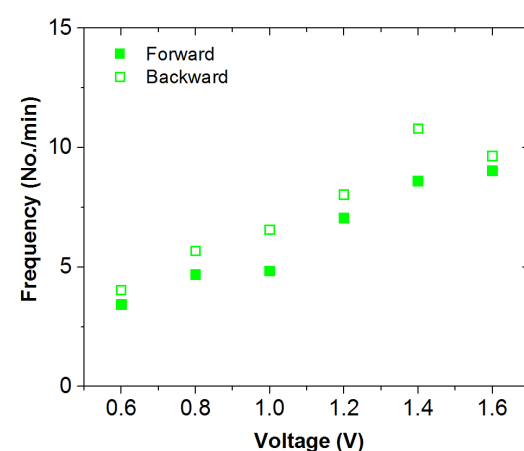


**Figure S8.** Number of charged 410 nm (left, blue symbols) and neutral 400 nm particles (right, green symbols) passing per minute through three micropores: (a) the same pore in Figures 1, 2; (b) the pore in Figure 3, and (c) the pore in Figure S4. Pore 3 was used only to detect charged 410 nm particles. The charged particles had an average zeta potential of  $-33 \pm 2$  mV at 100 mM KCl, pH 10.

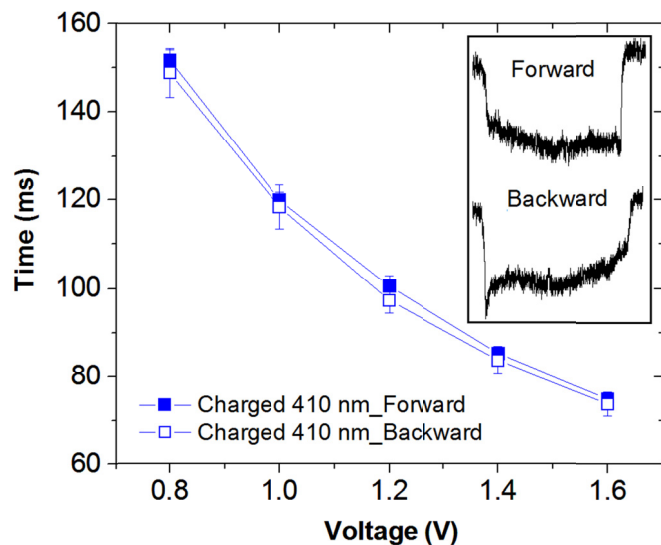


**Figure S9.** Passage time of charged 410 nm particles through a single 35  $\mu\text{m}$  long PET pore with an average opening diameter of 0.9  $\mu\text{m}$ . This pore was characterized by small diameter undulations, as suggested by the small fluctuations of ion current within the pulse. The particles had an average zeta potential of  $-33 \pm 2$  mV at 100 mM KCl, pH 10.

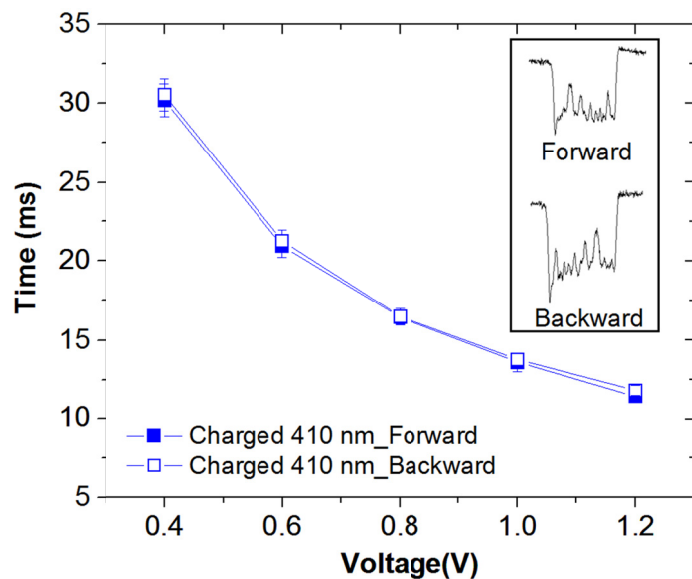


**Figure S10.** Passage times of charged 410 nm particles (zeta potential of  $-33 \pm 2$  mV at 100 mM KCl, pH 10) through an 11  $\mu\text{m}$  long PET pore with an average diameter of 0.9  $\mu\text{m}$ .

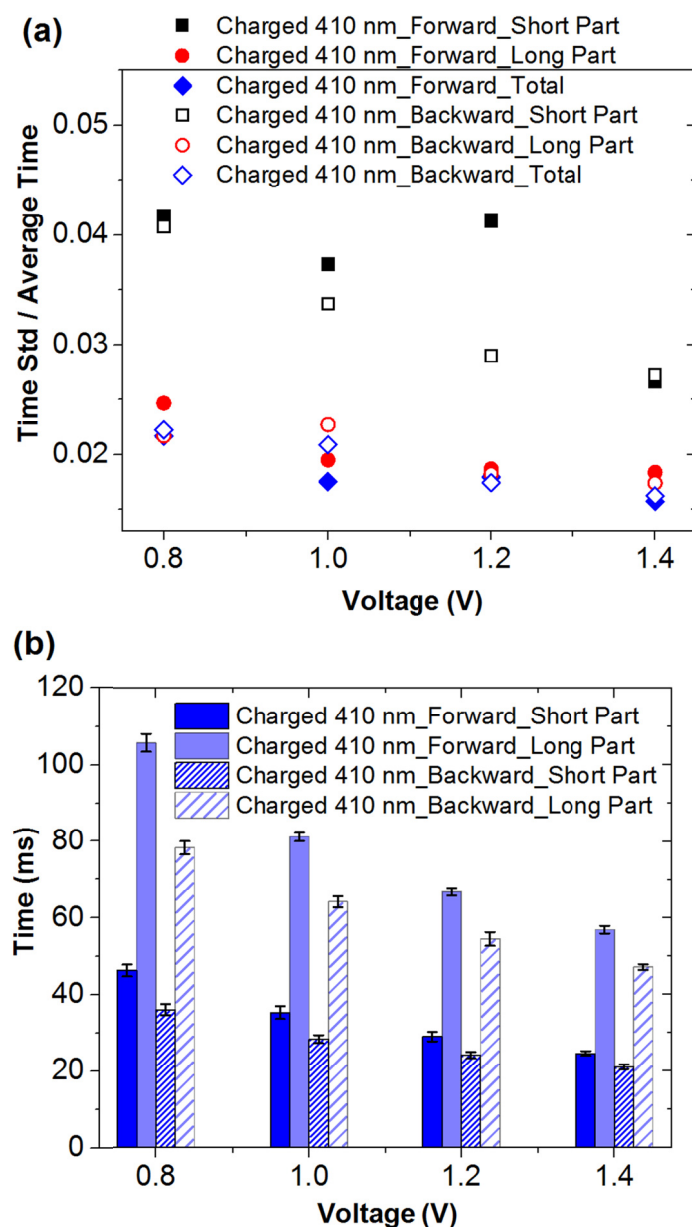


**Figure S11.** (a) Standard deviation of passage time for a pore shown in Figure 3 for charged 410 nm particles passing through two narrow zones of the pore (called Short Part and Long Part), and the total time (T); (b) Analysis of translocation times through the two narrower zones of the pore in Figure 3. Passage time in both directions is shown. Translocation time through the cavity of the same pore is analyzed in Figure 6 in the main manuscript.



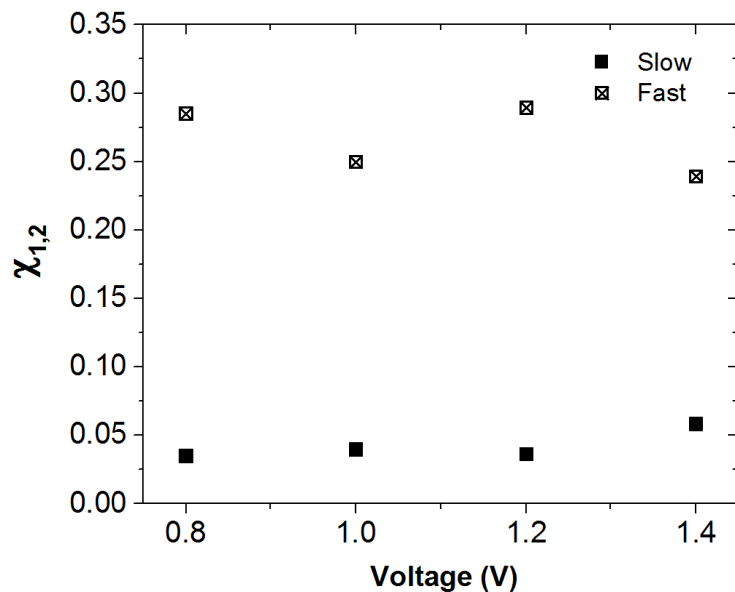


**Figure S12.** Magnitude of correlation coefficient  $\chi_{ij}$  (eq. (2) in the main manuscript) for data recorded for the pore shown in Figure 3 with charged 410 nm particles in the forward ('Slow') and backward ('Fast') directions as a function of voltage. The particles had an average zeta potential of  $-33 \pm 2$  mV at 100 mM KCl, pH 10.

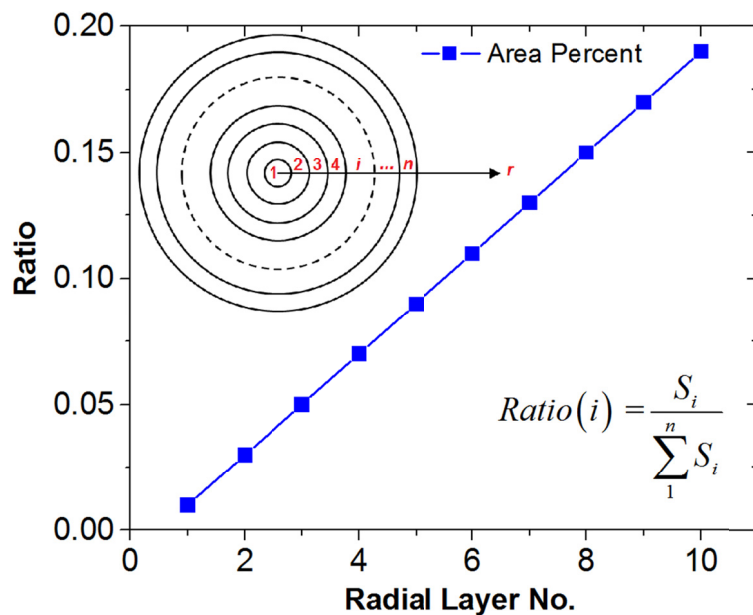


**Figure S13.** Ratio of an area of a layer (annulus) of a 1000 nm in diameter cylindrical pore and the total cross-section area. The pore was divided into 10 annuli with 50 nm widths.

## References

1. Qiu, Y.; Yang, C.; Hinkle, P.; Vlassiuk, I.V.; Siwy, Z.S. Anomalous Mobility of Highly Charged Particles in Pores. *Anal. Chem.* **2015**, *87*, 8517-8523.
2. Menestrina, J.; Yang, C.; Schiel, M.; Vlassiuk, I.; Siwy, Z. S. Charged Particles Modulate Local Ionic Concentrations and Cause Formation of Positive Peaks in Resistive-Pulse-Based Detection. *J. Phys. Chem. C* **2014**, *118*, 2391-2398.